

Nazar: Monitoring and Adapting ML Models on Mobile Devices

Wei Hao
Columbia University

Zixi Wang
Columbia University

Lauren Hong
Columbia University

Lingxiao Li
Columbia University

Nader Karayanni
Columbia University

Chengzhi Mao
Columbia University

Junfeng Yang
Columbia University

Asaf Cidon
Columbia University

Abstract

ML models are increasingly being pushed to mobile devices, for low-latency inference and offline operation. However, once the models are deployed, it is hard for ML operators to track their accuracy, which can degrade unpredictably (e.g., due to data drift). We design Nazar, the first end-to-end system for continuously monitoring and adapting models on mobile devices without requiring feedback from users. Our key observation is that often model degradation is due to a specific root cause, which may affect a large group of devices. Therefore, once Nazar detects a consistent degradation across a large number of devices, it employs a root cause analysis to determine the origin of the problem, and applies a cause-specific adaptation. We evaluate Nazar on two computer vision datasets, and show it consistently boosts accuracy compared to existing approaches. On a dataset containing photos collected from driving cars, Nazar improves the accuracy on average by 15%.

1 Introduction

Companies such as Google, Meta, Apple and LinkedIn, are increasingly running their ML models *on users' mobile devices*, so they can run inference locally at a low latency, even when the device is offline. Examples include text suggestion [18, 55], ranking posts, object detection and tracking for virtual reality [69], speech recognition [50] and targeted advertising [67]. As state-of-the-art ML models are very large, they are typically trained in the companies' datacenters with fleets of GPUs [53, 69]. A team of *ML operators* is usually responsible for retraining the models and pushing new model versions to the users' mobile devices.

However, in large-scale settings, ML operator teams lack sufficient visibility into the performance of the ML models running on users devices [59]. Model accuracy across devices is highly variable over time, and can change due to unexpected shifts in the input data (termed *data drift*) or hardware issues in specific devices (e.g., low-quality cameras, microphones) [19, 53]. Although the ML operators may fine-tune or retrain models to improve accuracy, it is quite difficult today to detect data drift in the first place or verify whether accuracy

has been restored properly after fine-tuning [53, 59–61]. The crux is that after the models are deployed, the ML operators have no “ground truth” on how accurate their models are because users do not manually label data.

Although many algorithms from the ML literature can detect data drift [28, 30–32, 38, 39, 42, 44, 48, 54, 63, 64], and adapt to the drifts [41, 45, 56, 62, 70], they often operate with impractical assumptions (e.g., assume fully-labeled data, or a single source of data drift, or require significant computational resources or manual inspection), and have never been tested in a real end-to-end system.

We present Nazar, the first end-to-end system for continuously monitoring and addressing data drift in large-scale ML deployments on mobile devices. We explicitly design Nazar to operate fully automatically without human involvement so that it can practically support large-scale ML deployments. It consists of three main functions: (a) automatically *detect* when data drift occurs on mobile devices, (b) *analyze* the root cause of the data drift, and (c) *adapt* to the cause that triggered the data drift, all without requiring any user input. Given that user-labeled data is not available and that operators have little resources for manual diagnosis, Nazar employs *self-supervised* methods for detecting, analyzing, and adapting to data drift, which we elaborate further below.

Detection. After considering a wide range of detection algorithms, we decided to adopt a *confidence threshold* method that detects data drift by comparing the model's confidence of the predictions against a threshold. This method requires no user-labeled data or manually supplied surrogate models, and is thus suitable for Nazar's automation requirement while providing good accuracy. Moreover, it is computationally lightweight and can easily work locally on any mobile devices.

Root cause analysis. A classical approach [10, 13] for root cause analysis is called *frequent itemset mining*, which finds sets of attributes (in our case, root causes) that are tied with specific data types (detected data drift). While this approach is useful in uncovering causes of drift, it leads to many duplicate root causes, which are subsets of or overlap with each other, and therefore is often used in settings in which a human manually inspects the results and acts upon them [10]. It is

untenable in large-scale settings that Nazar targets. Hence, we introduce novel *set reduction* and *counterfactual analysis* algorithms, two heuristics that automatically produce a small set of likely data drift root causes by eliminating root causes that subsume each other and overlap.

By-cause adaptation. The vast majority of existing adaptation techniques assume labeled data, and even those that do not, make completely impractical assumptions. They assume a single source of data drift, and adapt the model on each newly-arriving input [66, 71], which leads to poor accuracy when there are multiple sources of drift. Instead, we propose a novel *by-cause* model adaptation method, which selectively adapts the model only to the specific cause of accuracy degradation with the data that is suspected to have it.

The three Nazar components work harmoniously together, continuously reinforcing each other in an end-to-end loop. As our experiments show, Nazar’s analysis accurately identifies the root cause of the drift, so that by-cause adaptation is applied only to data drifted for the same cause. Otherwise, a model adapted to one cause is unlikely to have high accuracy on data that drifted due to completely different causes. Once an adapted model is deployed, Nazar’s detection will leverage the new model’s confidence to detect drifts, continuously improving accuracy. These components together enable Nazar to effectively obtain a consistently and significantly higher accuracy than existing approaches that adapt on all inputs, without requiring any manual work.

We implement Nazar on Amazon AWS, and evaluate it on two streaming datasets: cityscapes, a self-driving car dataset composed of images taken from driving vehicles in various European cities [20], and an ImageNet-derived dataset that emulates a species classification app. Nazar provides an average of 15% and up to 22% of accuracy boost on all data and an average of 19% and up to 50% on drifted data compared to the baselines on cityscapes. We will open source our datasets and code upon publication.

Our main technical contributions are:

1. First end-to-end online system for model monitoring and adaptation for mobile devices.
2. Fully-automated root cause analysis mechanism that introduces set reduction and counterfactual analysis to effectively narrow down the root causes of model degradation.
3. New self-supervised adaptation technique that adapts by root cause, which provides a significant accuracy boost over existing approaches when deployed with Nazar’s effective root cause analysis, without any human input.

2 Background and Related Work

Companies are increasingly deploying models on user devices for faster inference and to support low connectivity settings. On-device models support a wide range of use cases, including object recognition [69], text auto-complete [18, 55] and

ranking posts and ads [67, 69].

Where to train the models? These models can be trained either centrally in the cloud, or in a distributed fashion across the devices themselves (termed *federated learning*). The advantages of training the model in the cloud are: (a) the model training and evaluation process is simpler, and (b) powerful datacenter-based AI compute capabilities (e.g., a large number of GPUs/TPUs) are available for training. An advantage of federated learning is that it does not require uploading training data to the cloud, facilitating better privacy. While federated learning has seen increased interest both in academia [23, 27, 36, 37] and in industry [18, 55, 67], in this work, we primarily focus on the more common scenario, where the models are trained in the cloud. Nazar’s principles and ideas can also be applied to the federated learning case.

Model compression and quantization. Conducting inference on devices introduces several significant challenges. Since mobile devices are quite heterogeneous, and may impose significant resource limitations, models need to be adapted to be run on those devices. Several systems attempt to address this challenge, including TensorFlow Lite [8], an extension to TensorFlow that adapts trained models to resource-limited devices (e.g., using quantization). Another example is Mistify [24], which automatically adapts the model’s architecture to fit the device’s constraints.

Accuracy degradation. However, techniques like model compression can introduce subtle changes in the models, which may degrade their accuracy. These discrepancies in accuracy across devices can impact the applications’ quality of service [19, 53], and lead to security vulnerabilities [26, 53]. For example, while quantization can reduce the model size exponentially to fit on resource-constrained devices, it can also lead to worse accuracy for specific classes [19]. This accuracy degradation is hard to anticipate in advance.

Data drift. Data drift is a classic problem that affects models that operate on streaming data, where the distribution of the newly-arriving data diverges from training data’s distribution [22, 46, 68]. Data drift can occur for many reasons: temporal environmental changes or corruptions affecting the model input (e.g., weather, noise), changes in the input distribution itself (e.g., a self-driving model trained in the US might not recognize street signs in India), and sensor-related issues (e.g., problems with device microphone or camera lens). To deal with this problem, models are often frequently retrained with fresh data, even if some older data is retained, so their training data better reflects the types of inputs they will encounter during inference [14, 49]. The data drift problem is exacerbated in on-device deployments, because: (a) different devices may see divergent data distributions, and (b) when retraining in large-scale deployments, it is not feasible to re-

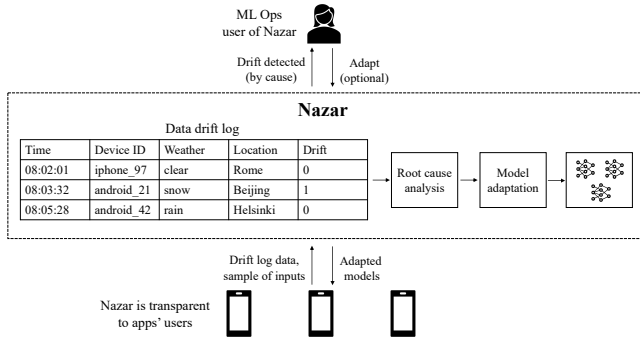


Figure 1: Nazar’s design.

train on data from *all devices*. Therefore, one needs to decide when to retrain and which devices to sample from.

Ekya [14] is a recent system that tackles a variant of this problem, by jointly scheduling retraining and inference on the same “edge” servers. In the case of Ekya, an edge server is a server with multiple GPUs sitting at the network’s edge (e.g., in a content distribution network), unlike our setting where inference is done on resource-constrained mobile devices. A second key difference is that, unlike Nazar, Ekya assumes labels are available for adapting the models.

Lack of visibility and monitoring. There are several efforts to provide more visibility and monitoring in ML pipelines. ML-EXray [53] is a framework that helps “debug” models by allowing ML operators to instrument logs and debugging assertions. It targets pre-processing issues, quantization bugs, and suboptimal kernels. Another data validation system for ML pipelines implemented at Meta [58] tries to identify possible attributes that caused model performance drop, from the training input. In contrast to these systems, Nazar focuses on post-deployment issues caused by data drift, while these systems focus more on the pre-deployment validation setting.

In summary, while there are existing systems that identify problems in models pre-deployment, and existing ad-hoc detection and adaptation techniques, to the best of our knowledge there is no automated end-to-end system for monitoring and adapting models on mobile devices.

3 Design

3.1 Overview

We present an overview of Nazar’s design (Figure 1). We design Nazar to be an end-to-end system that can automatically monitor data drift, identify the main root causes for the drift, and adapt models to them at scale, while dynamically evolving with changing data distributions in the real world.

Usage modes. The user of Nazar is the ML ops team, which maintains and retrains models. ML ops can choose their level

of interaction with Nazar: by default, Nazar runs in an “autopilot” mode, where monitoring, analysis and adaptation are all done automatically. The ML ops team can choose to more closely interact with the system, receiving alerts when data drift occurs, and manually deciding when to trigger the adaptation and on which root causes to apply them.

On-device detection. App users (i.e., users of the apps that run the AI models) are completely oblivious to Nazar. Nazar operates in the cloud, and interacts with the on-device models using an API. The apps contribute two types of information to Nazar. First, each time the models conduct inference, they also subsequently run a very lightweight drift detection algorithm (described in §3.2). The result of this algorithm, along with additional metadata about the device and model (e.g., the device’s ID, current location, local time, model version) are sent to Nazar in the cloud. We call this metadata collected from the devices a *drift log entry*. Second, periodically, in the background, the device will sample some percentage (by default 1%) of the inputs to the model, and send them to the cloud for model adaptation purposes.

Root cause analysis. The drift log entries are ingested into a database in the cloud, called the *drift log*. Periodically, Nazar runs a *root cause analysis* algorithm (§3.3). The algorithm is composed of: (a) a series of database queries on the data drift log to identify potential sets of causes of data drift, and (b) *set reduction* and *counterfactual analysis* algorithms, which reduce redundant causes and rank them to select the most important ones to adapt to. When drift is indeed detected, Nazar generates an alert for the ML ops team.

By-cause adaptation. After drift is detected, Nazar generates new *by-cause model adaptations* that adapt to the specific root causes of the drift (§3.4). These adaptations are pushed to the app users’ devices and used for new inferences. Since model updates can accumulate, Nazar consolidates the different versions to capture the relevant root causes with a small number of model adaptations. For inference, the device chooses which model version to use for each input, by selecting the one with attributes that best match the input.

Evolving drift detection. In the process of detecting, analyzing and adapting to drift, the concept of what is non-drift and what is drift evolves over time. If Nazar adapts on a certain source of drift, it should not continue to be detected as drift over and over again. Therefore, ideally the detector and root cause analysis should keep “adapting” to the new distribution of data, and only exhibit a high detection rate if they see data that diverges from the data the original model was trained on and that Nazar adapted its models to.

Design principles. The main questions in designing Nazar is how to design its detection, root cause analysis and adaptation mechanisms. Two primary principles guide our design:

1. As Nazar is transparent to app users, it requires *self-supervised* methods that cannot rely on labeled data.
2. Nazar must support fully-automated operation, without relying on the ML ops team instruction.

3.2 On-Device Data Drift Detection

We now describe Nazar’s data drift detector, which runs on the mobile devices. The goal of the data drift detector is to detect when data drift has occurred on a particular device in a lightweight fashion, without requiring any user input.

3.2.1 Data Drift Detection Techniques

When designing Nazar’s drift detection mechanism, we considered different data drift (also known as “concept drift” and “out-of-distribution drift”) algorithms from the ML literature. However, most of these techniques were not designed for an on-device inference setting. Table 1 summarizes the eight primary techniques we evaluated. We introduce the classes of techniques, and describe our rationale for focusing on methods that are derived from the model’s inference output.

Detecting based on model output. One class of data drift detection techniques assumes that data drift is correlated with the model being “unsure” about the correct class to output. Therefore, they apply various metrics on the model’s *logit* vector (or un-normalized log probabilities). As a refresher, in deep neural network (DNN) models, the model outputs an array that assigns a probability for each class. Typically the highest scoring class is chosen as the predicted class. The distribution of this vector can indicate how “certain” a model is about its prediction. For example, the MSP *threshold* [30] checks if the maximum softmax value of the logit vector is below a certain threshold. If it is, the model is uncertain about the final prediction, which is correlated with data drift. Prior work also proposes other types of thresholds or metrics, such as the entropy of the softmax values [64] and other similar scores [44]. In our experiments, we found these thresholds to perform almost identically to MSP. MSP has the small advantage that it is normalized between 0 and 1, making it a simpler knob to tune, and hence we adopt it. The advantage of this class of algorithms is that they can simply be applied to the model’s inference output with negligible computational overhead (since the logit scores are anyways computed by the inference), and do not require any outside information.

Statistical test on batch of outputs. Orthogonal to the aforementioned methods that use a simple threshold for data drift detection, statistical tests can be combined with any of these scores to determine whether the inference data diverges from the training data distribution [64]. For example, Kolmogorov-Smirnov (KS) test (KS-test in Table 1) compares the empirical cumulative distribution functions (CDFs) of the

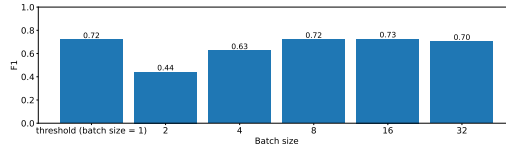


Figure 2: Comparison of F1 scores using KS-test with different batch sizes. For batch size is 1, we use threshold on MSP with default value 0.9.

two datasets and calculates their maximum difference. Prior work [54] conducts empirical studies on using different combinations of statistic test and finds that applying KS-test on softmax outputs yields the best detection accuracy. Hence, this is the main statistical test we evaluate.

External datasets. Another class of methods assumes training-time access to a dataset that contains drifted data samples. The intuition is that such a “drift dataset” will help train a model to be more sensitive to all drifts. Examples include Outlier-Exposer [31] (OE in Table 1), Odin [42] and Mahalanobis Distance [39] (MD). We deem these approaches impractical for our setting, because our data is unlabeled, and we cannot assume that users will prepare drift datasets which is a meaningless concept for a user.

Secondary model. Some techniques employ auxiliary models to detect data drift. SSL [32] and CSI [63] co-train an auxiliary model for self-supervised tasks on a transformed version of the dataset (e.g., they rotate images in the original dataset and perform rotation angle classification). The assumption is that if there was no drift, after training, both models would have high confidence on the same input. We rule out this class of methods, given that some mobile devices are resource constrained, and we cannot rely on them to invoke an additional model purely for data drift detection.

Methods that require backpropagation. Generalized Odin [34] (GOdin) is an expanded version of Odin that does not require the use of a secondary dataset but requires adding small adversarial perturbations to make the model more confident when data is in distribution, and less confident when data has drifted. However, to add these perturbations, it requires an extra step of *backpropagation* after the softmax values are read, i.e., the neural network needs to be traversed in reverse. Unfortunately backpropagation cannot be used in certain compressed models, which means this technique would not be usable for many types of adapted models pushed to user devices.

3.2.2 Chosen Detection Technique: Threshold on MSP

After ruling out most of the techniques due to their lack of fit with on-device inference, we finalize a shortlist of two detection methods: the simple MSP threshold method that operates on one model-outputted logit vector at a time, and the KS-test statistical method, which operates on a batch of

	Threshold [30]	KS-test [54]	OE [31]	Odin [42]	MD [39]	SSL [32]	CSI [63]	GOdin [34]
No secondary dataset	✓	✓	✗	✗	✗	✓	✓	✓
No secondary model	✓	✓	✓	✓	✓	✗	✗	✓
No backpropagation	✓	✓	✓	✗	✓	✓	✓	✗
No batching	✓	✗	✓	✓	✓	✓	✓	✓

Table 1: Comparison of different data drift detection algorithms from the ML literature. Nazar uses the threshold method, which simply applies a threshold on the model’s softmax output, such as the max softmax score.

MSP scores. To evaluate these methods we measure their *F1 score* to compare their effectiveness on an equal split of clean and drifted images (described in §5.3) and a ResNet50 model (see §5.2) is used to generate the logit vectors. The F1 score is defined as:

$$F1 = 2 \cdot \frac{\text{Precision} \cdot \text{Recall}}{\text{Precision} + \text{Recall}} = 2 \cdot \frac{TP}{2TP + FP + FN} \quad (1)$$

where a high score indicates that the detector has a good balance between precision and recall. In other words, the model is able to correctly identify true positives (the image is “drifted”, i.e., it belongs to a different distribution than the training set, and the detector thinks it is drifted) while minimizing false positives (the image is not drifted and the detector thinks it is drifted) and false negatives (the inverse). For the KS-test method, we test it with different batch sizes and assign the detection result (i.e., a boolean value for drift or non-drift) *on the whole batch*. For the threshold method, we set its default value to 0.9 (we evaluate this choice in §5.3).

Figure 2 displays the results, showing that when the batch size is higher than 4, KS-test slightly outperforms the threshold method, but is worse when the batch size is lower. However, batching results from device inference raises various tricky questions: should one batch inference results from a specific device over time? How long should we allow that time window to be? How do we batch results when we do not have sufficient samples from a single device to fit in one batch?

Since the threshold method performs very similarly to KS-test with large batches, and since using a batched detection method raises these thorny issues, we choose the threshold method with MSP as the default detection module in Nazar.

3.3 Root Cause Drift Analysis

As we will show later (§5), since the drift detection algorithm operates without any user input or labeled data, and it is simply a function of the model’s uncertainty, the detection algorithm is somewhat noisy for each individual detection. Therefore, we need a more accurate mechanism at a system level to determine whether drift has actually occurred, and why. This subsection explores the design of this mechanism, which we call the *root cause drift analysis*.

In Nazar, for each inference, the device sends to the cloud the data drift detection results, as well as metadata about the device and its environment (e.g., weather and geolocation, as depicted by the example in Table 2). Each entry is called the

Time	Device ID	Weather	Location	Drift
06:02:01	android_42	clear-day	Helsinki	False
06:02:23	android_21	clear-day	New York	False
06:04:55	android_21	clear-day	New York	True
08:03:32	android_21	snow	New York	True
11:05:01	android_42	snow	Helsinki	True

Table 2: Example of drift log.

drift log entry, and the entries are assembled in a single large database in the cloud, called the *drift log*. Hence, the drift log is a live global view of data drift across all devices.

We walk through the algorithm using a toy example of two devices (one in New York, one in Helsinki) running an application for classifying animals in their natural settings. This application produces a drift log (Table 2). Each device generates a few drift entries, which contain metadata on the current location of the device and the weather it is operating in. This metadata can be either gleaned by the device itself (e.g., its location) or generated by Nazar in the cloud via an external source (e.g., for weather metadata, Nazar looks up the weather in a third-party weather API using the device’s location). In this example, the root cause of the drift is the snowy weather, which transforms the image sufficiently so that it diverges from the original training data – imaged taken in clear days – used to train the model. The example includes a false positive drift detection, i.e., the third entry in the log, where the detection threshold algorithm marked the image as “drifted” (due to low confidence logit scores), even though the image was not.

Frequent itemset mining (FIM). To identify whether drifts exist and discover its root causes in the face of potential false positives and negatives, Nazar focuses only on clusters of drifts that are statistically significant. One possible approach is to directly apply an ML-based clustering algorithm on the entries flagged as drifts. We did not adopt this approach because clustering algorithms often require specifying how many clusters to divide the data into (e.g., the *K* parameter in K-means), and can be expensive, especially at scale [57].

An alternative, classical data mining approach [11, 12] is to explore whether sets of attributes in the drift log entries, e.g., {snow, New York} in Table 2, frequently appear with the drift attribute. These attributes are termed in the data mining literature as *frequent itemsets* and there exist many algorithms [12, 16, 17, 25, 51, 52] for frequent itemsets mining (FIM).

In the first stage of root cause analysis, shown in Fig-

Rank	Occurrence	Support	Risk Ratio	Confidence	Weather	Location	Location
0	0.4	0.67	3	1	snow	-	-
1	0.2	0.3	2	1	snow	-	android_21
2	0.2	0.3	2	1	snow	-	android_42
3	0.2	0.3	2	1	snow	New York	-
4	0.2	0.3	2	1	snow	Helsinki	-
5	0.4	0.7	1.3	0.67	-	-	android_21
6	0.4	0.7	1.3	0.67	-	New York	-
7	0.4	0.7	1.3	0.67	-	New York	android_21
8	0.2	0.33	0.75	0.5	-	-	android_21
9	0.2	0.33	0.75	0.5	-	-	android_42
10	0.2	0.33	0.75	0.5	-	Helsinki	-
11	0.2	0.33	0.75	0.5	clear-day	-	android_21
12	0.2	0.33	0.75	0.5	-	Helsinki	android_42
13	0.2	0.33	0.75	0.5	clear-day	New York	-
14	0.2	0.33	0.75	0.5	-	Helsinki	-
15	0.2	0.33	0.33	0.33	clear-day	-	-

Table 3: Example of frequent itemset mining results.

ure 3(a), Nazar implements an FIM mechanism that employs the *apriori algorithm* [13]. The apriori algorithm is a common method for FIM, which first identifies frequent individual attributes in the entry and then uses them to generate larger sets of attributes associated with the drift attribute. The algorithm calculates several metrics starting from sets containing each single attribute, and then the sets containing combinations of attributes which form subsets of the single ones, e.g., {snow, New York} is a subset of {snow}. It filters the sets by checking if statistics from the metrics pass certain thresholds to consider a certain set as a cause of drift, since the drift detection is noisy. Finally, it ranks which sets of attributes are the leading causes of drift. The metrics and ranking for the example drift log in Table 2 are shown in Table 3.

The *occurrence* of a set of attributes measures how often it appears in the drift log. The *support* of a set of attributes measures how often it is marked as “drift” as a proportion of all log entries that are marked as drifted. E.g., {snow} has a support of 0.67, because $\frac{2}{3}$ of the drift entries have the attribute “snow”. The *confidence* of an attribute set is how often it is marked as drift as a proportion of all its appearances in the table. Finally, the *risk ratio* of a set measures how much likelier entries that are marked as drifted contain the set of attributes versus not containing it. E.g., for {snow, Helsinki}, the risk ratio is 2, because the probability of an entry being drift given it contains {snow, Helsinki} is 1 and the probability of an entry being drift given it does not contain {snow, Helsinki} is $\frac{1}{2}$.

By default, Nazar uses the risk ratio to rank the results, because it measures the importance of a specific root cause. Following prior work [10], Nazar sets the maximum number of attributes that can belong to a single root cause to 3, and uses values of 0.01, 0.01, 0.51 and 1.1 for minimum occurrence, support, confidence and risk ratio respectively, by default.

Practical limitations of FIM. While FIM is a useful technique to rank root causes and set some thresholds on which root causes are important, systems that rely on it typically assume that a human will then inspect the results and manually choose the appropriate root causes [10]. In our example in Table 3, the top seven rows are all possible root causes,

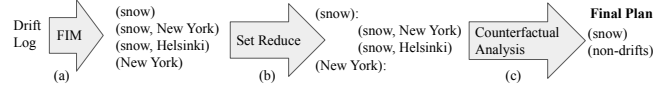


Figure 3: Flow of root cause analysis.

since they pass the four thresholds. However, it would not be a good idea to simply adapt models to each one of these root causes, since they are overlapping and even contain subsets of each other (e.g., {snow, New York} is a subset of {snow}). Therefore, Nazar needs a way to narrow down this set of possible root causes so it can apply model adaptations sparingly, covering as many relevant root causes as possible without requiring operator instruction.

Set reduction. There are two types of possibly redundant root causes that may have already been addressed in other root causes, and thus can be *reduced*. First, a root cause which is a subset of other root causes that have broader coverage. For example, {snow, New York} is a subset of both {snow} and {New York}, so if one of these two is selected as root causes for model adaptations, there is no reason to select their intersection, e.g., {snow, New York}. Nazar’s set reduction algorithm merges the subset root cause into one of its supersets that has higher ranking, e.g., {snow, New York} is merged into {snow} instead of {New York}, because {snow} is ranked higher (rank 0). This stage is termed as *set reduction* and is depicted in Figure 3(b).

Counterfactual analysis. The second cause of redundancy is overlapping causes, when the entries with drift are already “covered” by some other root causes. In our example, $\frac{2}{3}$ entries from New York contain drift signals though $\frac{1}{3}$ are false positives. However, this subset of images is already addressed by a higher-ranked root cause, e.g., {snow}. Nazar filters out this type of root cause by applying counterfactual analysis [40], which iteratively modifies the drift attribute from the log entries associated with a higher-ranked root cause to be “false”, and tests whether the lower-ranked root cause is still statistically significant by checking the four metrics after these drift attributes have been modified. If it is still statistically significant, Nazar add this lower-ranked root cause into the final result. Note that the first top-ranked root cause is directly added to the final result. This iterative process is shown in Figure 3(c) and it runs until all root causes from the set reduction output are exhausted. Eventually, Nazar groups images associated with each filtered root cause, e.g., images that have “snow” in their meta-data. Note that Nazar also filters a set of images that are “clean” when they are not associated with previously discovered root causes. Algorithm 1 summarizes the root cause analysis mechanism.

Limitations. The primary limitation of our root cause analysis is that the drift log attributes may not capture all possible root causes of drifts. For example, certain devices may have

Algorithm 1 Root cause analysis algorithms

$FIM()$:

Output: Extracts frequent sets of attributes associated with drift.

$Set_Reduction(FIM_table)$:

Input: Sorted list of attribute sets.

Output: Mapping between the most coarse-grained attribute sets and their subsets. Ties between coarse-grained sets are broken by ranking.

$Passes_Drift_Threshold(items)$:

Input: Attribute set potentially causing drift.

Output: True if the set passes thresholds (occurrence, support, confidence, and risk). False otherwise.

Drift Analysis:

```
1:  $FIM\_list \leftarrow FIM()$ 
2:  $coarse\_associations \leftarrow Set\_Reduction(FIM\_list)$ 
3:  $root\_causes \leftarrow []$ 
4: while  $coarse\_associations$  do
5:    $curr\_coarse\_cause \leftarrow coarse\_associations.pop()$ 
6:   if  $Passes\_Drift\_Threshold(curr\_coarse\_cause)$  then
7:      $root\_causes.append(curr\_coarse\_cause.key)$ 
8:      $Mark\_No\_Drift(curr\_coarse\_cause.key)$ 
9:   else
10:    for each  $subset$  in  $curr\_coarse\_cause.value$  do
11:      if  $Passes\_Drift\_Threshold(subset)$  then
12:         $root\_causes.append(subset)$ 
13: return  $root\_causes$ 
```

camera lenses from a particular manufacturer that are causing image corruption, but the drift log might not contain an attribute of the lens manufacturer for each device. In such cases, Nazar may group devices by their models, their location, or even by device ID, even though the “real” root cause is the lens. In such cases, Nazar should still automatically produce by-cause adaptations, which would capture these data drifts, but the ML operator team would have to manually investigate the issue in order to understand the real root cause. To combat this issue, in large-scale settings, the list of attributes should be exhaustive, to capture unforeseen causes of drift.

3.4 By-Cause Adaptation

Most model adaptation techniques [41, 45, 56, 62, 70] and end-to-end ML systems that incorporate adaptation (e.g., SageMaker [43], TFX [47]) require labeled data, which are unsuitable for our design.

We focus on two main self-supervised methods for adapting models to data drift, motivate the idea of adapting a model to a *specific cause of drift*, and introduce how Nazar chooses different adapted model versions for inference.

Self-supervised adaptation. Nazar’s model adaptation builds on prior work on self-supervised adaptation. The intuition is to select a self-supervised objective (e.g., minimize the entropy of the model output) that captures some invariant of the data itself without requiring any labels. Upon data drift, this objective is no longer optimal, therefore we can

optimize the model weights to minimize this objective again, effectively adapting the model to the drift.

We consider two methods: TENT [66] and MEMO [71]. TENT adapts any pre-trained probabilistic model by minimizing the entropy on the logits output by the model, on a batch of images. MEMO adapts on marginal entropy, which is the entropy of the averaged output logits, over different augmented copies of a single image, e.g., by rotating and posterizing the image. The idea is that the model should be (a) invariant across augmented versions of the image, and (b) confident in its predictions even for heavily-augmented versions of the image.

We make three modifications to these methods to make them practical for the setting of large ML deployments on mobile devices that Nazar targets. First, both methods tightly couple adaptation and inference: they adapt the models based on the current inference inputs, and then immediately run inference on the inputs. However, as discussed in §2, many mobile devices are too wimpy for on-device adaption, so we decouple adaption and inference in Nazar. Second, MEMO adapts a whole model including all its layers, significantly increasing network consumption and model storage costs because each adaptation leads to a whole new version of the model weights. We thus modify MEMO to adapt only the *batch normalization (BN) layer* [35], similar to TENT. As an example, in ResNet50 the BN layer is $217\times$ smaller than the full model (0.4MB vs. 92MB). Our experiments show that adapting only the BN layer in MEMO has the same accuracy boost as adapting all layers. Third, we modify MEMO to adapt based on a small batch of inputs instead of on every input because the latter would be impractical in our setting, incurring too frequent adaptations even for one-off or falsely-detected drifts.

Benefit of adapting by cause over adapting blindly.

Prior adaption methods unrealistically assume a single cause behind the data drift and adapt on all inputs, but in practice data drift can originate from different sources: for example, a traveler may bring her device from location to location over a short period of time, experiencing very different input distributions each corresponding to a different cause (location). We show in our experiments below that adapting by cause improves model performance significantly over adapting blindly on all inputs. Moreover, to illustrate the need for accurate root cause analysis, we show that a model adapted to one cause of data drift has poor performance when applied to data that is drifted due to a different cause or non-drifted (i.e., clean) data.

We adapt a pre-trained ResNet50 on a dataset that contains 16 different types of data drifts, such as weather-based corruptions and image blur (§5 describes the evaluation setup), and a portion of clean data. We run TENT and MEMO in two settings: (a) adapt and test a model for each cause of drift and clean data (17 total models), termed *by-cause*, and (b) adapt

Methods	Average Accuracy (%)
No-adapt	38.7
By-cause (TENT)	61.5
By-cause (MEMO)	42.3
Adapt-all (TENT)	42.4
Adapt-all (MEMO)	30.3

Table 4: TENT and MEMO when adapting them by-cause, and using a single model to adapt to all sources.

one model on a mix of all 16 sources of drifts and clean data, and test them on the same test set as in (a), termed *adapt-all*. We also evaluate non-adapted ResNet50 on the same test set.

The average test accuracy is shown in Table 4. Adapting on data by-cause using both methods improves accuracy over the original model, by 22.8% for TENT and 3.6% for MEMO; whereas adapting on all the data degrades accuracy with MEMO and leads to small gains with TENT. The reason is that adapting models to multiple divergent distributions without supervision can cause models to underfit and leads to low performance. To further demonstrate this, we run an experiment where we adapt a model by-cause (foggy weather), and test it on images with other sources of drift. On average, the model obtains an average accuracy of only 16.4% when run on images with other sources of drift, and an accuracy of 66.7% on its own test set. Its accuracy on clean data is also very low: 26.8%, while the model adapted on clean data has an accuracy of 74.6% on the same clean test set.

Therefore, we conclude that Nazar has to adapt its models sparingly and apply them carefully; it should apply adapted models only when there is a true prevalent source of data drift that affects some portion of user devices, and ideally run the resulting adapted model on data that experiences the same source of drift. These observations motivate Nazar to adapt different models by distinct root cause, so that the distribution of inference data will be as close as possible to the one of the training data. Ideally, each by-cause adapted model should run inference on data that belongs to the same distribution it was adapted on, while a continuously adapted “clean” model should be run on clean data. Since no ground truth exists, Nazar has to rely on its root cause analysis to determine which devices are experiencing data drift and from which source. In addition, this motivates us to use TENT as the default method to adapt the models in Nazar, since TENT largely outperforms MEMO in the both strategies in our experiment, as shown in Table 4. However, ML operators are free to use any self-supervised adaptation method with Nazar.

Consolidating model versions. Adapting by-cause generates multiple model versions. We cannot allow the number of models to grow unbounded, especially on resource-constrained devices. Nazar constrains the number of models that can be stored on each user device, by periodically consolidating them. To consolidate different versions, Nazar keeps a global view of the model pool, in a least recently updated

(LRU) list, which contains the sets of models to be deployed. The oldest models make room for the newer ones. Orthogonally to the LRU algorithm, if a new model version belongs to the exact same set of attributes as an existing one, the older one is evicted without having to evict the tail of the LRU. In addition, if an incoming model version has a root cause that is a superset of an older model version, the older version gets evicted (similar to the set reduction algorithm in §3.3).

Picking which model to use for inference. During inference on the device, Nazar will use the most-recently updated model that has the highest number of matching attributes for inference, e.g., {rain, New York} has more attributes matching than {rain} if the input image is associated with {rain, New York}. It uses the risk ratio ranking of a root cause, described in §3.3, to break ties between model versions. If no matching model is found, it uses its “clean” model for inference. Note that model selection for inference is run on the device without any involvement from the cloud.

4 Implementation

We now describe our prototype implementation of Nazar on Amazon AWS. To support a large number of devices and models, our implementation uses highly-scalable AWS services. Such services exist on all cloud providers, and our implementation could be easily ported to other clouds.

Drift log. We run the drift log on Amazon Aurora [65], a relational database that supports over 120,000 writes per second and can be scaled to 128 terabytes. The drift log is stored as a table, where each row contains the metadata and whether the inference was detected as a data drift.

Root cause analysis and adaptations. The root cause analysis is run periodically as an Amazon Lambda function, which is triggered either automatically based on a configurable time window or manually by the ML operator. The FIM algorithm is run as a set of SQL queries on the drift log. The initial phase of the algorithm requires extracting the attributes frequently associated with drift. This can be implemented using a simple SQL COUNT aggregation, with appropriate conditions. The function then calculates the FIM metrics, which are used to filter and rank the root causes. The function then runs the set reduction and counterfactual analysis. Finally, each narrowed-down root cause is sent to a GPU-equipped instance, which conducts the adaptation by-cause.

5 Evaluation

This section answers the following questions:

- Q1:** How well does Nazar’s detection algorithm detect different types of data drift? (§5.3)

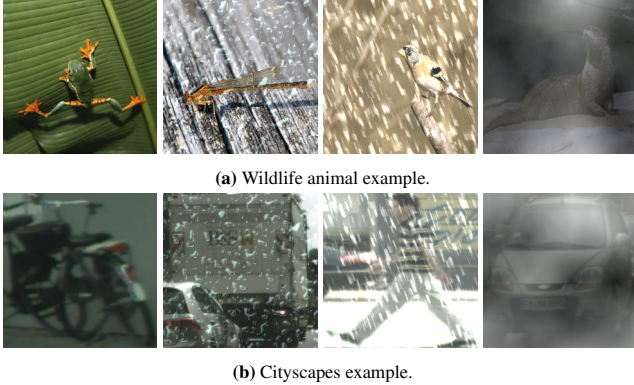


Figure 4: Examples of clean image and images with rain, snow and fog (corruption severity of 3) from the two datasets.

- Q2:** How effective is Nazar’s root cause analysis in identifying the root cause of drift? (§5.4)
- Q3:** How does by-cause adaptation perform compared to prior approaches? (§5.5)
- Q4:** Does the detector evolve with model adaptation? (§5.6)
- Q5:** What is the accuracy gain in end-to-end workloads? (§5.7)
- Q6:** How quickly does Nazar adapt to data drift and how well does the root cause analysis scale? (§5.8)

We first describe our datasets (§5.1) and our experimental setup (§5.2), and then answer the evaluation questions.

5.1 Datasets

Our evaluation uses two configurable datasets: cityscapes and animal wildlife, which represent the datasets of two typical applications of Nazar. Both datasets are emulated over a period between January 1st 2020 and April 21st, 2020, following a Kaggle dataset of historical weather [5], which exhibits dynamic weather patterns. We apply synthetic weather-based data drifts (rain, snow and fog) based on the historic weather for different locations using data from a weather website [9]. By default, we evenly divide the time for both datasets by 8, and run Nazar after each interval. The drifts are applied as different types of random corruptions to the images. We parameterize the severity of different data drifts and the probability of an image experiencing them under the corresponding weather condition. By default, we set this probability to 1. For example, if an image from Hamburg is tagged to have been generated on January 18th, 2020, and the historical weather for that day indicated there was rain at some point during that day, by default, we apply a drift function for rain (e.g., see Figure 4) on that image.

Cityscapes. A potential application of Nazar is in driver automation and self-driving car models, which conduct on-device object classification and image segmentation [15]. Similar to prior work (Ekya [14]), we prepare an object detection dataset for a self-driving car application, built on top of the

cityscapes dataset, which contains photos of traffic-related objects collected from driving cars from 50 cities in Europe [20]. Following Ekya’s methodology, we pre-process cityscapes for object classification, resulting in 27,604 images, and use 14% of the dataset for the initial training, 6% for validation and 80% for streaming new inferences. Since photos in each city are associated with sequence numbers, we assume users submit them based on their original order. We assume the dataset at each location starts at January 1st, 2020 and ends at April 21st, 2020, and that the images are submitted for inference in equal intervals across these dates.

Animals. In addition to cityscapes, which is a temporally-tagged dataset, we also generate a parameterized synthetic dataset that would allow us to methodologically configure our system. For this dataset we are inspired by iNaturalist [6], an application for nature lovers to tag animals in the wild, which uses object classification to help users identify animal species in seconds. We emulate a geodistributed deployment of iNaturalist, where subscribers from different locations are taking photos and attempting to identify different animal species in the wild. We build this dataset on top of a subset of the classes from ImageNet [4], which contains 201 classes of animals excluding pets. Each one of these classes contains on average 793 images for model training, 50 images for validation, and 500 images for streaming. We did not use the established iNaturalist [33] because both the distribution shift functions and adaptation methods were designed and tested for ImageNet [29, 66, 71] and we want to conduct a fair comparison between Nazar and prior adaptation approaches.

We emulate 7 locations from different continents: New York, Tibet, Beijing, New South Wales, United Kingdom and Quebec, where each location contains a different distribution of animal species. Each location contains a configurable number of user devices with a configurable arrival pattern of inference requests. By default, we set the number of devices to 16 for each location and the request pattern to be a Poisson distribution with a mean of two images per day per device.

Class skew. We introduce another source of data drift, *class skew*. We observe that a model’s accuracy of images from different classes varies (Figure 5b), even though the number of training images for each class is similar. Therefore, if a certain location exhibits a higher proportion of images from lower-accuracy classes, the model’s accuracy may suffer. To emulate this effect, we generate the distribution of classes for each location by randomly assigning probabilities for each class under the Zipf distribution, where the higher the Zipf parameter α is, the more skewed the class distribution. By default, we set α to be 0 (uniform) but also evaluate under a high skew ($\alpha = 1$).

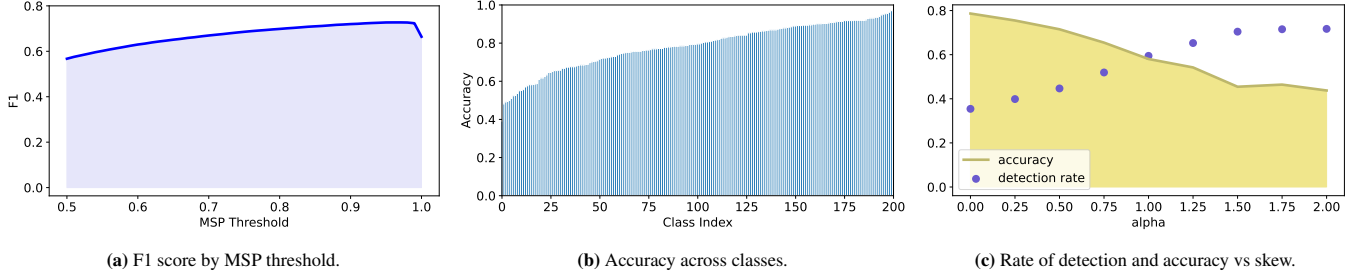


Figure 5: 5a shows F1 scores of MSP detector are fairly stable on different threshold values. 5b shows average accuracy on different animal classes is highly variable. 5c shows the accuracy decreases and detection rate increases when skew is high.

Analysis Methods / Ground Truth Drifts	None	Rain	Snow	Fog	Fog & Snow	Fog & Rain	Snow & Rain	Snow & Rain & Fog
FIM	1	0.919	0.773	1	0.891	0.921	0.926	0.917
FIM with Set Reduction	1	0.919	0.773	1	0.891	0.921	0.934	0.919
FIM with Set Reduction and CF Analysis	1	1	0.874	1	1	1	1	1

Table 5: Evaluation of root cause analysis algorithms with Fowlkes-Mallows Score (1 is optimal).

5.2 Evaluation Setup

AWS setup. Our AWS implementation uses the following configurations. The drift log is run on Amazon Aurora [65] with a 5.7.mysql_aurora.2.11.1 engine on a db.r6g.2xlarge instance [2]. The drift analysis is run as an AWS Lambda [3] serverless function with 256MB of memory. The adaptation is run on a p3.2xlarge EC2 instance, which is equipped with an NVIDIA Tesla V100 GPU [1].

Models. We use three image classification models in all experiments, ResNet18, ResNet34 and ResNet50, which are commonly-used model architectures for mobile devices [7]. Each model is trained from scratch until convergence. The accuracy of each model on clean (non-drifted) validation dataset with cityscapes is 83.6%, 83.9% and 83.7%, respectively, while the accuracy of the base model on the animal dataset is 72.1%, 75.4% and 76.1%.

Data drifts. Prior work on drifts apply 16 types of different data drift on ImageNet [29]. In microbenchmarks in §5.3, §5.5 and §5.6 we show how Nazar handles all 16 types of drifts. Our end-to-end evaluation (§5.7) contains only the three weather-related drifts (snow, rain, fog), as the distribution of weather is dynamic and driven by real historical weather records. 29% and 36% of days in the cityscape and animal datasets, respectively, experience weather-related drifts. All 16 drifts use a severity level of 3 (out of 5) by default.

Baselines. We compare Nazar with two other settings: adapt-all, which is the baseline approach (e.g., employed by Eky, TENT, MEMO), where one model is continuously adapted on all input during each adaptation window, and no-adapt, which is a pre-trained model that is never adapted. Note that besides adapt-all, we also conducted experiments on TENT to adapt on only the images whose drift attribute is

“True” but this method always yields worse performance than adapt-all and thus we do not present its results here.

5.3 Detection (Q1)

To show how well the MSP threshold detects drifts, we measure the F1 scores calculated with different MSP thresholds on the logit outputs from Resnet50. We evenly applied 16 types of drifts on half of the streaming images in the animal dataset, as the positive set, and leave another half non-drifted, as the negative set. We show the result in Figure 5a, where the F1 score of MSP detector steadily increases until it reaches 0.73 and then decreases. The detector’s sensitivity to threshold changes is small around a threshold of 0.9, which we adopt as a default value.

Further illustrating this point, in Figure 5c, we vary the class skew, i.e., we vary the distribution we sample from different classes, where under high skews we are much likelier to sample specific animal classes than others. The result shows that the detector rate significantly increases and the total accuracy degrades under high class skew.

These results indicate that the MSP threshold is a good indicator of different sources of drifts.

5.4 Root Cause Analysis (Q2)

We evaluate Nazar’s root cause analysis using the Fowlkes-Mallows Score (FMS) [21], which measures the similarity between two sets of clustering results. In our case, the two sets are ground truth root causes of drift, and ones that are identified by our root cause analysis. The FMS score is:

$$FMS = \sqrt{\frac{TP}{TP+FP} \cdot \frac{TP}{TP+FN}} \quad (2)$$

where TP (true positive) is the number of pairs of data points that are clustered together in both sets, FP (false positive) is

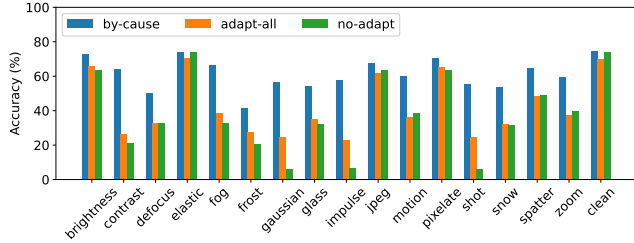


Figure 6: Experiments of by-cause, adapt-all, and no-adapt on 16 different drifted data and clean data

the number of pairs that are clustered together in the second set but not in the first, and FN (false negative) is the inverse of FP. The score ranges from 0 to 1, with higher values indicating more similarity between the clusters. We use 8 drift scenarios, depicted in Table 5, whose ground truth root causes of drifts are different combinations of three weather corruptions on the animal dataset for 14 days starting on January 1st, 2020, on a ResNet50. As an example, if the ground truth root causes are “fog” and “snow” then we apply only these two types of drifts on the dates that have foggy and snowy weather for each location but ignore “rain” drift on the rainy days.

The combination of FIM, set reduction, and counterfactual analysis always yields the highest score under each scenario. In fact, it obtained the optimal FMS score under all drift scenarios except “snow”.

5.5 Adaptation (Q3)

To evaluate whether by-cause adaptation performs better than the naive approach, i.e., adapting on all coming images, we evenly split the images in the animal dataset in 17 partitions, 16 of which are transformed with different drifts, and one is left as clean, and run them on ResNet50. To isolate the performance of the adaptation mechanism, we assume perfect knowledge of the underlying root cause of the data drift, and that we adapt only to images with that root cause (i.e., we assume Nazar’s detector and root cause analysis are perfect). We treat the clean data as its own data source, and run an adaptation model for it as well.

Figure 6 breaks down the average accuracy by drift type. By-cause adaptation significantly and consistently outperforms the adapt-all. In addition, it provides a significant improvement compared to the baseline non-adapted model, while adapt-all sometimes degrades the accuracy of the non-adapted model. The total average accuracy increase of by-cause adaptation in this experiment is very significant: it achieves a 61.5% accuracy, compared to only 42.4% for adapt-all and 38.7% for the non-adapted model.

We conclude that by-cause adaptation shows promise in overcoming the limitations of traditional supervised adaptation approaches, paving the way for more scalable and efficient adaptation in real-world applications.

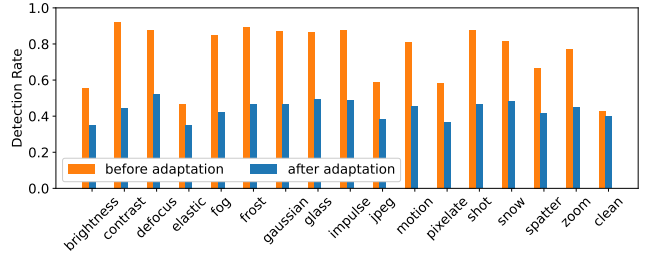


Figure 7: Detection rate before and after adaptation.

5.6 Evolving Drift Detection (Q4)

We test how the by-cause adaptation influences the drift detector. Using the same experimental setup as the previous subsection, Figure 7 displays the detection rate for each one of the drift types before adaptation and after adaptation. The after adaptation detection rate is measured for the adapted model that matches the drift type of the input image. The results show two interesting insights. First, before adaptation the detector is rather accurate in catching most of the sources of drift, but has some noise. Second, when it uses the appropriately adapted model, it is less likely to detect the data as drift, and exhibits the same detection probability for drifted data and clean data. Therefore, Nazar is not expected to frequently detect root causes again once it has adapted to them.

5.7 End-to-End Workloads (Q5)

We now evaluate all components of Nazar end-to-end on our streaming workloads. We first evaluate the general performance on the cityscapes dataset and then test them on the more synthetic animal dataset under more severe drift conditions, i.e., higher severity for weather drifts and class skew.

Average accuracy. We measure the average accuracy on all data averaged across the last 7 time windows on the cityscapes dataset in Figure 8a. For all model architectures, Nazar yields the highest average accuracies and the smallest standard deviations. The improvements in average accuracy compared with adapt-all are very significant: 10.1–19.4%.

We also measure the average accuracy of only the drifted data averaged across three types of data drift in Figure 8b, which shows even more significant accuracy improvements compared to adapt-all (49.5% on ResNet18 and 37.6% on ResNet34), which is because smaller models have a weaker ability to generalize on a mixed source of distributions.

Figure 8c shows the cumulative average accuracy over time for all data and only for drifted images. The cumulative accuracy of Nazar continuously improves over time with each adaptation window, while the one for adapt-all increases for one adaptation window, as the drift level is mild even in the no-adapt case, and then decreases in the following 3 adaptation windows, after which they slightly increase. This demonstrates

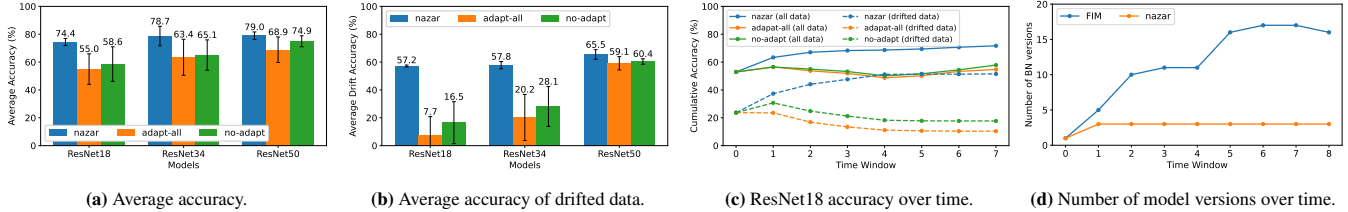


Figure 8: Results of experiments on cityscapes dataset. 8a and 8b show the average accuracy on all data and drifted data under three strategies. 8c shows the trace of accumulated accuracy per time window. 8d shows the number of model versions on user devices when set reduction and counterfactual analysis are removed from Nazar.

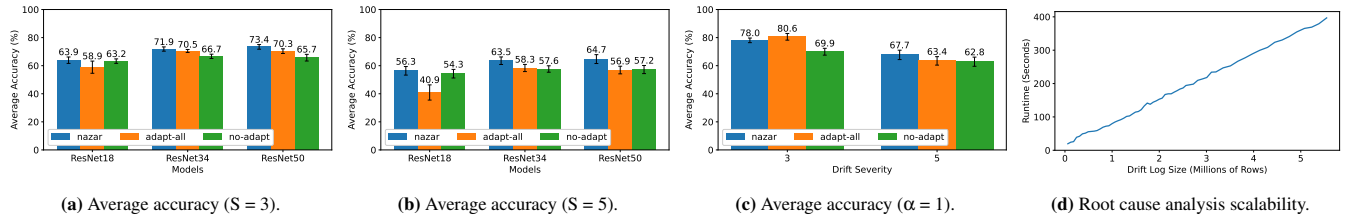


Figure 9: Results of experiments on Animals dataset. 9a and 9b show the average accuracy with different drift severities under three strategies. 9c shows the average accuracy with class skew of $\alpha=1$. 9d shows the scalability of Nazar’s root analysis function.

the utility of adapt by-cause, which provides much more stable accuracy over time, both for clean and drifted data.

Benefit of set reduction and counterfactual analysis. To find out if the set reduction and counterfactual analysis are effective in the end-to-end setting, we only run the FIM algorithm for root cause analysis, and find the average accuracy drops 1.3–9.7%. Meanwhile, the number of stored BN versions (recall we only adapt the BN layer, so each BN layer represents a different adapted model) is much higher than Nazar, due to the redundant root causes. We show an example of the numbers of BN versions, from ResNet18, stored on user devices during each time window for FIM and Nazar in Figure 8d, where the number of BN versions with Nazar is steady at 3 from the second time window. Note in this experiment we do not cap the number of model versions for Nazar.

Adaptation frequency. We evaluate if the number of adaptation cycles affects adaptation performance. We ran the end-to-end workloads by splitting them into 4 intervals instead of 8, and found the results stayed very consistent. The average accuracy across the three models improved by 1.2–3.8%.

Drift severity. We vary the severity of the corruptions on the animal dataset (Figure 9a and 9b), where a higher severity represents a higher level of drift, and severity is denoted by “S”. When severity is higher, all three methods degrade on both accuracy metrics but Nazar still outperforms among them. Nazar’s improvements compared to adapt-all is larger when the severity is higher (3.8–10.4% better).

Class skew. We evaluate the effect of class skew on Nazar with ResNet50, by setting the Zipfian parameter $\alpha = 1$. The

results are presented in Figure 9c. Nazar fails to outperform adapt-all on average accuracy when severity is set to 3 on the animal dataset, because Nazar has a narrower view of diverse image features than adapt-all, when the variability of classes in each location is largely constrained by class skew, and thus tends to overfit the model during adaptation. When we increase the variety of images during each adaptation by splitting the workload into 4 intervals instead of 8, Nazar outperforms both baselines and improves the average accuracy of 0.9% compared with adapt-all. In addition, when the severity is higher, Nazar yields better average accuracy even when the number of time windows is 8, also shown in Figure 9c which offsets the impact from class skew.

5.8 Runtime and Scalability (Q6)

Runtime. Once a sufficient number of entries contain data drift, Nazar should be able to generate adaptations in a reasonably timely manner to respond to the drift. We measure the latency of Nazar from the invocation of the root cause analysis function, through the model adaptations and up until the adapted models are written S3, and repeat the experiment four times. The average end-to-end latency is 49.5 minutes. The average root cause analysis runtime is only 46 seconds, while the rest of the time is consumed by the model adaptation. Note that this time can be shortened by adding additional or larger adaptation instances.

Scalability. Nazar’s three components are designed to be highly scalable. The drift log relies on a scalable database (Aurora), and model adaptation can be easily parallelized on a large number of instances. Thus, the only component that could potentially become a scalability bottleneck is the root cause analysis function, since a single function needs

to operate on a relatively large number of Aurora rows via a series of SQL queries. Figure 9d presents the runtime of the root cause analysis running on a single instance, as a function of the drift log size. We can see the relationship between the runtime and the number of rows in the drift log is completely linear. The reason is that the FIM algorithm is linear [13] and the number of candidate sets of attributes is greatly reduced for counterfactual analysis after the set reduction.

6 Conclusions

Nazar is the first end-to-end monitoring and adaptation system for mobile-based ML deployments. We conclude that chaining together drift detection run on the device, with root cause analysis and by-cause adaptation run in the cloud, provides high accuracy, even without user input. Interesting avenues for future work are adapting Nazar to distributed federated learning, and developing techniques for better protecting user privacy.

References

- [1] Amazon EC2 P3 instances. <https://aws.amazon.com/ec2/instance-types/p3/>. Accessed: April 27, 2023.
- [2] Amazon RDS instance types. <https://aws.amazon.com/rds/instance-types/>. Accessed: April 27, 2023.
- [3] AWS Lambda. <https://aws.amazon.com/lambda/>. Accessed: April 27, 2023.
- [4] ImageNet Object Localization Challenge. <https://www.kaggle.com/c/imagenet-object-localization-challenge>, 2017.
- [5] Historical daily weather data 2020. <https://www.kaggle.com/datasets/vishalvjoseph/weather-dataset-for-covid19-predictions>, 2020. Accessed: Apr 12, 2021.
- [6] iNaturalist. <https://www.inaturalist.org/>, 2023.
- [7] Pytorch android examples. <https://github.com/pytorch/android-demo-app>, 2023. Accessed: May 3, 2023.
- [8] TensorFlow Lite. <https://www.tensorflow.org/lite>, 2023.
- [9] Weather underground. <https://www.wunderground.com/>, 2023. Accessed: Mar 8, 2023.
- [10] ABUZAID, F., KRAFT, P., SURI, S., GAN, E., XU, E., SHENOY, A., ANANTHANARAYAN, A., SHEU, J., MEIJER, E., WU, X., NAUGHTON, J., BAILIS, P., AND ZAHARIA, M. DIFF: A relational interface for large-scale data explanation. *Proc. VLDB Endow.* 12, 4 (dec 2018), 419–432.
- [11] AGRAWAL, R., IMIELIŃSKI, T., AND SWAMI, A. Mining association rules between sets of items in large databases. In *Proceedings of the 1993 ACM SIGMOD International Conference on Management of Data* (New York, NY, USA, 1993), SIGMOD '93, Association for Computing Machinery, p. 207–216.
- [12] AGRAWAL, R., MANNILA, H., SRIKANT, R., TOIVONEN, H., VERKAMO, A. I., ET AL. Fast discovery of association rules. *Advances in knowledge discovery and data mining* 12, 1 (1996), 307–328.
- [13] AGRAWAL, R., SRIKANT, R., ET AL. Fast algorithms for mining association rules. In *Proc. 20th int. conf. very large data bases, VLDB* (1994), vol. 1215, Santiago, Chile, pp. 487–499.
- [14] BHARDWAJ, R., XIA, Z., ANANTHANARAYANAN, G., JIANG, J., KARIANAKIS, N., SHU, Y., HSIEH, K., BAHL, V., AND STOICA, I. Eky: Continuous learning of video analytics models on edge compute servers. *CoRR abs/2012.10557* (2020).
- [15] BOJARSKI, M., TESTA, D. D., DWORAKOWSKI, D., FIRNER, B., FLEPP, B., GOYAL, P., JACKEL, L. D., MONFORT, M., MULLER, U., ZHANG, J., ZHANG, X., ZHAO, J., AND ZIEBA, K. End to end learning for self-driving cars. *CoRR abs/1604.07316* (2016).
- [16] BORGELT, C. Efficient implementations of apriori and eclat. In *FIMI'03: Proceedings of the IEEE ICDM workshop on frequent itemset mining implementations* (2003), Citeseer, p. 90.
- [17] BORGELT, C. An implementation of the fp-growth algorithm. In *Proceedings of the 1st international workshop on open source data mining: frequent pattern mining implementations* (2005), pp. 1–5.
- [18] CHEN, M., MATHEWS, R., OUYANG, T., AND BEAUFAYS, F. Federated learning of out-of-vocabulary words. *arXiv preprint arXiv:1903.10635* (2019).
- [19] CIDON, E., PERGAMENT, E., ASGAR, Z., CIDON, A., AND KATTI, S. Characterizing and taming model instability across edge devices. *Proceedings of Machine Learning and Systems* 3 (2021).
- [20] CORDTS, M., OMRAN, M., RAMOS, S., REHFELD, T., ENZWEILER, M., BENENSON, R., FRANKE, U., ROTH, S., AND SCHIELE, B. The cityscapes dataset for semantic urban scene understanding. *CoRR abs/1604.01685* (2016).
- [21] FOWLKES, E. B., AND MALLOWS, C. L. A method for comparing two hierarchical clusterings. *Journal of the American statistical association* 78, 383 (1983), 553–569.
- [22] FRENCH, R. M. Catastrophic forgetting in connectionist networks. *Trends in cognitive sciences* 3, 4 (1999), 128–135.
- [23] GHOSH, A., CHUNG, J., YIN, D., AND RAMCHANDRAN, K. An efficient framework for clustered federated learning. *Advances in Neural Information Processing Systems* 33 (2020), 19586–19597.
- [24] GUO, P., HU, B., AND HU, W. Mistify: Automating DNN model porting for on-device inference at the edge. In *NSDI* (2021), pp. 705–719.
- [25] HAN, J., PEI, J., AND YIN, Y. Mining frequent patterns without candidate generation. *ACM sigmod record* 29, 2 (2000), 1–12.
- [26] HAO, W., AWATRAMANI, A., HU, J., MAO, C., CHEN, P.-C., CIDON, E., CIDON, A., AND YANG, J. A tale of two models: Constructing evasive attacks on edge models. *Proceedings of Machine Learning and Systems* 4 (2022), 414–429.
- [27] HE, C., LI, S., SO, J., ZENG, X., ZHANG, M., WANG, H., WANG, X., VEPAKOMMA, P., SINGH, A., QIU, H., ET AL. FedML: A research library and benchmark for federated machine learning. *arXiv preprint arXiv:2007.13518* (2020).
- [28] HEIN, M., ANDRIUSHCHENKO, M., AND BITTERWOLF, J. Why relu networks yield high-confidence predictions far away from the training data and how to mitigate the problem. *CoRR abs/1812.05720* (2018).
- [29] HENDRYCKS, D., AND DIETTERICH, T. G. Benchmarking neural network robustness to common corruptions and perturbations. *CoRR abs/1903.12261* (2019).
- [30] HENDRYCKS, D., AND GIMPEL, K. A baseline for detecting misclassified and out-of-distribution examples in neural networks. *CoRR abs/1610.02136* (2016).
- [31] HENDRYCKS, D., MAZEIKA, M., AND DIETTERICH, T. G. Deep anomaly detection with outlier exposure. *CoRR abs/1812.04606* (2018).
- [32] HENDRYCKS, D., MAZEIKA, M., KADAVATH, S., AND SONG, D. Using self-supervised learning can improve model robustness and uncertainty. *CoRR abs/1906.12340* (2019).

- [33] HORN, G. V., AODHA, O. M., SONG, Y., CUI, Y., SUN, C., SHEPARD, A., ADAM, H., PERONA, P., AND BELONGIE, S. The inaturalist species classification and detection dataset. In *CVPR* (2018).
- [34] HSU, Y., SHEN, Y., JIN, H., AND KIRA, Z. Generalized ODIN: detecting out-of-distribution image without learning from out-of-distribution data. *CoRR abs/2002.11297* (2020).
- [35] IOFFE, S., AND SZEGEDY, C. Batch normalization: Accelerating deep network training by reducing internal covariate shift. *CoRR abs/1502.03167* (2015).
- [36] LAI, F., DAI, Y., SINGAPURAM, S., LIU, J., ZHU, X., MADHYASTHA, H., AND CHOWDHURY, M. FedScale: Benchmarking model and system performance of federated learning at scale. In *International Conference on Machine Learning* (2022), PMLR, pp. 11814–11827.
- [37] LAI, F., ZHU, X., MADHYASTHA, H. V., AND CHOWDHURY, M. Oort: Efficient federated learning via guided participant selection. In *15th USENIX Symposium on Operating Systems Design and Implementation (OSDI 21)* (July 2021), USENIX Association, pp. 19–35.
- [38] LEE, K., LEE, H., LEE, K., AND SHIN, J. Training confidence-calibrated classifiers for detecting out-of-distribution samples. *arXiv preprint arXiv:1711.09325* (2017).
- [39] LEE, K., LEE, K., LEE, H., AND SHIN, J. A simple unified framework for detecting out-of-distribution samples and adversarial attacks. In *NeurIPS* (2018).
- [40] LEWIS, D. *Counterfactuals*. John Wiley & Sons, 2013.
- [41] LI, Z., AND HOIEM, D. Learning without forgetting. *IEEE transactions on pattern analysis and machine intelligence* 40, 12 (2017), 2935–2947.
- [42] LIANG, S., LI, Y., AND SRIKANT, R. Principled detection of out-of-distribution examples in neural networks. *CoRR abs/1706.02690* (2017).
- [43] LIBERTY, E., KARNIN, Z., XIANG, B., ROUESNEL, L., COSKUN, B., NALLAPATI, R., DELGADO, J., SADOUGHI, A., ASTASHONOK, Y., DAS, P., ET AL. Elastic machine learning algorithms in amazon sagemaker. In *Proceedings of the 2020 ACM SIGMOD International Conference on Management of Data* (2020), pp. 731–737.
- [44] LIU, W., WANG, X., OWENS, J. D., AND LI, Y. Energy-based out-of-distribution detection. *CoRR abs/2010.03759* (2020).
- [45] MALTONI, D., AND LOMONACO, V. Continuous learning in single-incremental-task scenarios. *Neural Networks* 116 (2019), 56–73.
- [46] MCCLOSKEY, M., AND COHEN, N. J. Catastrophic interference in connectionist networks: The sequential learning problem. In *Psychology of learning and motivation*, vol. 24. Elsevier, 1989, pp. 109–165.
- [47] MODI, A. N., KOO, C. Y., FOO, C. Y., MEWALD, C., BAYLOR, D. M., BRECK, E., CHENG, H.-T., WILKIEWICZ, J., KOC, L., LEW, L., ZINKEVICH, M. A., WICKE, M., ISPIR, M., POLYZOTIS, N., FIEDEL, N., HAYKAL, S. E., WHANG, S., ROY, S., RAMESH, S., JAIN, V., ZHANG, X., AND HAQUE, Z. Tfx: A tensorflow-based production-scale machine learning platform. In *KDD 2017* (2017).
- [48] NGUYEN, A. M., YOSINSKI, J., AND CLUNE, J. Deep neural networks are easily fooled: High confidence predictions for unrecognizable images. *CoRR abs/1412.1897* (2014).
- [49] PARISI, G. I., KEMKER, R., PART, J. L., KANAN, C., AND WERMTER, S. Continual lifelong learning with neural networks: A review. *Neural networks* 113 (2019), 54–71.
- [50] PAULIK, M., SEIGEL, M., MASON, H., TELAAR, D., KLUIVERS, J., VAN DALEN, R., LAU, C. W., CARLSON, L., GRANQVIST, F., VANDEVELDE, C., ET AL. Federated evaluation and tuning for on-device personalization: System design & applications. *arXiv preprint arXiv:2102.08503* (2021).
- [51] PEI, J., HAN, J., MAO, R., ET AL. Closet: An efficient algorithm for mining frequent closed itemsets. In *ACM SIGMOD workshop on research issues in data mining and knowledge discovery* (2000), vol. 4, pp. 21–30.
- [52] PEI, J., HAN, J., MORTAZAVI-ASL, B., PINTO, H., CHEN, Q., DAYAL, U., AND HSU, M.-C. Prefixspan: mining sequential patterns efficiently by prefix-projected pattern growth. In *Proceedings 17th International Conference on Data Engineering* (2001), pp. 215–224.
- [53] QIU, H., VAVELIDOU, I., LI, J., PERGAMENT, E., WARDEN, P., CHINCHALI, S., ASGAR, Z., AND KATTI, S. ML-EXray: Visibility into ML deployment on the edge. *Proceedings of Machine Learning and Systems* 4 (2022), 337–351.
- [54] RABANSER, S., GÜNNEMANN, S., AND LIPTON, Z. Failing loudly: An empirical study of methods for detecting dataset shift. *Advances in Neural Information Processing Systems* 32 (2019).
- [55] RAMASWAMY, S., MATHEWS, R., RAO, K., AND BEAUFAYS, F. Federated learning for emoji prediction in a mobile keyboard. *arXiv preprint arXiv:1906.04329* (2019).
- [56] REBUFFI, S.-A., KOLESNIKOV, A., SPERL, G., AND LAMPERT, C. H. icarl: Incremental classifier and representation learning. In *Proceedings of the IEEE conference on Computer Vision and Pattern Recognition* (2017), pp. 2001–2010.
- [57] SCULLEY, D. Web-scale K-means clustering. In *Proceedings of the 19th international conference on World wide web* (2010), pp. 1177–1178.
- [58] SHANKAR, S., FAWAZ, L., GYLLSTROM, K., AND PARAMESWARAN, A. G. Moving fast with broken data. *arXiv preprint arXiv:2303.06094* (2023).
- [59] SHANKAR, S., GARCIA, R., HELLERSTEIN, J. M., AND PARAMESWARAN, A. G. Operationalizing machine learning: An interview study, 2022.
- [60] SHANKAR, S., HERMAN, B., AND PARAMESWARAN, A. G. Rethinking streaming machine learning evaluation. *arXiv preprint arXiv:2205.11473* (2022).
- [61] SHANKAR, S., AND PARAMESWARAN, A. G. Towards observability for machine learning pipelines. *CoRR abs/2108.13557* (2021).
- [62] SHMELKOV, K., SCHMID, C., AND ALAHARI, K. Incremental learning of object detectors without catastrophic forgetting. In *Proceedings of the IEEE international conference on computer vision* (2017), pp. 3400–3409.
- [63] TACK, J., MO, S., JEONG, J., AND SHIN, J. CSI: novelty detection via contrastive learning on distributionally shifted instances. *CoRR abs/2007.08176* (2020).
- [64] VAN LOOVEREN, A., KLAISE, J., VACANTI, G., COBB, O., SCILLITOE, A., AND SAMOILESCU, R. Alibi detect: Algorithms for outlier, adversarial and drift detection, 2019.
- [65] VERBITSKI, A., GUPTA, A., SAHA, D., BRAHMADESAM, M., GUPTA, K., MITTAL, R., KRISHNAMURTHY, S., MAURICE, S., KHARATISHVILI, T., AND BAO, X. Amazon Aurora: Design considerations for high throughput cloud-native relational databases. In *Proceedings of the 2017 ACM International Conference on Management of Data* (2017), pp. 1041–1052.
- [66] WANG, D., SHELHAMER, E., LIU, S., OLSHAUSEN, B. A., AND DARRELL, T. Fully test-time adaptation by entropy minimization. *CoRR abs/2006.10726* (2020).
- [67] WANG, E., KANNAN, A., LIANG, Y., CHEN, B., AND CHOWDHURY, M. FLINT: A platform for federated learning integration. *arXiv preprint arXiv:2302.12862* (2023).
- [68] WIDMER, G., AND KUBAT, M. Learning in the presence of concept drift and hidden contexts. *Machine learning* 23 (1996), 69–101.
- [69] WU, C.-J., BROOKS, D., CHEN, K., CHEN, D., CHOUDHURY, S., DUKHAN, M., HAZELWOOD, K., ISAAC, E., JIA, Y., JIA, B., ET AL. Machine learning at Facebook: Understanding inference at the edge. In *2019 IEEE International Symposium on High Performance Computer Architecture (HPCA)* (2019), IEEE, pp. 331–344.

- [70] YIN, X., YU, X., SOHN, K., LIU, X., AND CHANDRAKER, M. Feature transfer learning for deep face recognition with under-represented data. *arXiv preprint arXiv:1803.09014* (2018).
- [71] ZHANG, M., LEVINE, S., AND FINN, C. MEMO: test time robustness via adaptation and augmentation. *CoRR abs/2110.09506* (2021).